Estimating Interzonal Leakage in a Net-Zero Energy House

Lisa Ng[1], Lindsey Kinser[2], Steven Emmerich[1], Andrew Persily[1]

[1] Indoor Air Quality and Ventilation Group, Engineering Laboratory, National Institute of Standards and Technology, Gaithersburg MD
[2] College of Engineering, Mechanical Engineering and Mechanics, Drexel University

ABSTRACT

The Net-Zero Energy Residential Test Facility (NZERTF) was constructed at the National Institute of Standards and Technology (NIST) to support the development and adoption of cost-effective net-zero energy designs and technologies. The 250 m^2 two-story, unoccupied NZERTF, built in 2012, had among its design goals an airtight and highly insulated building enclosure designed for heat, air and moisture control. The airtightness goal was achieved through detailed envelope design, and careful construction, as well as during and after construction commissioning. When it was built, the NZERTF was one of the tightest residential buildings in North America with a whole building pressurization test result of roughly 0.6 h^{-1} at 50 Pa measured per ASTM E779-19, *Standard Test Method for Determining Air Leakage Rate by Fan Pressurization*. No special attention was given to the airtightness of the interior floors and other interior partitions. To support airflow modeling efforts, this interior leakage was quantified through a series of interzonal pressurization tests. Both the basement and attic were considered to be conditioned spaces because the thermal and air-moisture barriers encompass the basement walls and attic roof. Transfer grilles and other openings linked the living space to these two zones. A series of fan and partition configurations were used to quantify the leakage values of the various interzone airflow paths. Test results showed that the interior floors were more than 10 times leakier than the exterior building envelope and that the leakage associated with the transfer grilles between levels was less than the floor leakage. This paper describes the design of the interzonal tests and the challenges in

performing them, which included isolating zones, controlling multiple blower doors, and access for installing pressurization fans. The results of these tests were inputs to a multizone airflow (CONTAM) model of the building for use in evaluating the effects of different ventilation strategies and other airflow-related technologies on energy consumption and indoor air quality.

Keywords

airtightness, interzonal leakage, net-zero house, ASTM E779-10, pressurization tests

INTRODUCTION

In 2017, buildings were associated with 39 % of all energy used in the United States, with residential buildings and commercial buildings accounting for 20 % and 19 %, respectively [1]. Based on estimates by the U. S. Department of Energy (DOE), infiltration alone accounts for 14 % and 6 % of the energy used by residential and commercial buildings, respectively [2]. To reduce these energy impacts, tighter building envelopes are being required by codes and standards [2-5]. There are no standards related to the leakiness of interior floors and walls based on energy and indoor air quality considerations (though some fire codes address the issue), even though interzonal airflow through these surfaces can be important for contaminant transport and thus occupant exposure [6].

The literature on interzonal airflow experiments includes analyses of two-zone test cases [7-9]. Determining interzonal airflow is more difficult than whole building testing, either requiring a series of pressurization tests or multiple tracer gas tests. Emmerich et al. [7] conducted interzonal pressurization tests in five homes with attached garages to determine the leakiness of the house-garage interface. The tests involved placing one or two fans in different exterior doorways and altering the positions of the door connecting the two zones, as well as of the garage door to the outside. They found that the house-garage interface (normalized by the house-garage surface area) was two and half times to nearly eleven times leakier than the house exterior envelope (normalized by the house exterior surface area), which has implications for the transfer of contaminants from garages into houses. Hult et al. [9] compared the results of various single-fan and two-fan tests of the leakiness of house-garage interfaces. They also compared single-pressure difference to multiple-pressure difference tests. They found that a method using one fan in two configurations provided results with the smallest uncertainty among the single-fan tests. In general, the single-pressure tests led to less reliable results than the multiple-pressure tests. Though requiring an extra configuration, the "one-fan, three configurations" test performed by Emmerich et al. [7] also resulted in low uncertainty.

Tracer gas tests have also been used to determine interzonal airflow rates, as opposed to the interzone partition leakiness determined by the previously-described fan pressurization tests [10-15]. Du et al. [16] conducted constant-concentration tracer tests in several homes using two tracer gases. The steady-state concentrations of the tracer gases were used to estimate the airflow rates between a bedroom and the rest of the home. They found that most of the air entering the bedrooms came from somewhere else in the house and not from outside. Conversely, most of the air entering the rest of the house came from outside and not from the bedroom. They also found that homes that relied more on central heating and cooling systems had relatively higher interzonal airflows than homes in which occupants opened windows for ventilation.

This paper examines the use of blower door tests to determine the effective leakage area (ELA) of various house components (exterior envelope, interior floor leakage, leakage of transfer grilles) for input into a multizone airflow model. The results of such simulations can be used to evaluate different ventilation strategies and other airflow-related technologies to study the effects of weather, indoor conditions, and system operation on interzonal airflow and contaminant transport. This paper describes the test house, the design of the interzonal tests and the challenges in performing these tests, as well as the performance of a multizone airflow model (i.e., CONTAM) using measured values of interior leakages to predict contaminant concentrations. Interzonal tracer decay tests also were performed, and their analyses are saved for future work.

TEST HOUSE

The Net-Zero Energy Residential Test Facility (NZERTF) was built on the campus of the National Institute of Standards and Technology (NIST) in 2012 to demonstrate low-energy residential technologies with the goal of net-zero energy use on an annual basis (FIG. 1). The NZERTF is a 250 m^2 two-story, unoccupied house located in Gaithersburg, MD with an unfinished basement and an attic, both within the conditioned space. As reflected in TABLE 1, which summarizes the physical characteristics of the house, the basement is mostly below-grade, with a window well providing egress. A two-story foyer with a staircase connects the first and second floor, which has a horizontal area of approximately 17 m^2 (12 % of the first floor area). Given the open connection between these two floors, they were considered a single zone in these tests.

The detached garage contains the controls and data acquisition systems of the instruments and sensors in the NZERTF, so that their heat load is not introduced into the home. Lighting, appliances, plug loads, and sensible and latent heat loads of the simulated occupants are controlled by the data acquisition system [17]. A virtual family consisting of two adults and two children are simulated in the house, with their electrical and water usage varying over a seven-day schedule [18].

TABLE 1. Physical characteristics of NZERTF

Building characteristic	**Value**
Roof area	184 m^2
Basement wall area (above-grade)	2 m^2
First floor/second floor exterior wall area	314 m^2
Attic floor	130 m^2
Basement ceiling	151 m^2
Total exterior surface area	500 m^2
Total volume (basement, first floor, second floor, attic)	1300 m^3

The main design goal of the NZERTF was to achieve net-zero energy use over the course of a year, which was achieved from July 2013 to June 2014. One of the ways to reduce energy use in homes is to reduce heating and cooling loads because Since infiltration can account for 14 % of the total energy use of a home, the NZERTF was designed and constructed to be airtight. The building envelope airtightness of the NZERTF was tested to be 0.63 h^{-1} at 50 Pa [19], which is tighter than the requirements in LEED v4 [20] and ENERGY STAR v3.1 [21], and only slightly leakier than the Passive House U. S. requirement [22]. The normalized leakage (NL) value for the house equals 0.06, which is tighter than 99 % of U.S. homes based on statistical analysis of the Lawrence Berkeley National Laboratory Residential Diagnostics Database [23]. The NL value is defined in the ASHRAE Fundamentals Handbook [24] as follows:

$$NL = 1000 \left(\frac{ELA_4}{Area}\right)\left(\frac{H}{2.5\ m}\right)^{0.3} \qquad (1)$$

where ELA_4 (m^2) is the ELA at 4 Pa, Area (m^2) is the floor area, and H (m) is the house height.

FIG. 1. NZERTF at NIST facing south.

The basement, first floor, and second floor were actively conditioned by a central, air-source heat pump. The central heat pump had supplies in the basement, first floor, and second floor. Two returns were on the first floor and two returns were on the second floor. The heat pump has no outdoor air intake. Three transfer grilles were located on the floor of the first level to allow airflow between the basement and the house (referred to as the first floor transfer grilles). Two transfer grilles were located on the ceiling of the second floor to allow airflow between the attic and the house (FIG. 2a) referred to as the attic transfer grilles. Because the attic is within the thermal envelope, the attic transfer grilles were installed to provide the attic with conditioned air without requiring air distribution ductwork in the attic [25]. All the transfer grilles contain a damper that would close in case of a fire. The basement door and the attic hatch were closed during normal operation of the house. The basement door had an undercut that was approximately 0.9 m wide by

2.5 cm high, and the attic hatch door had a gap around it that was approximately 0.3 cm wide and 5.5 m long around its perimeter. Under depressurization, smoke tests were performed around interior airflow paths, such as the transfer grilles and around the basement door (FIG. 2) to better understand the airflow through these building elements. Smoke tests were also used to identify airflow paths that should be sealed during pressurization testing, such as the access panels in a bathroom used for signal and control wire (FIG. 2c) to isolate and determine leakage associated with the construction of the floors, basement door, and attic door. Other interior airflow paths that were sealed during testing included the supplies and returns of the central heat pump and the independently ducted mechanical ventilation system, the heat recovery ventilator (HRV). The HRV was balanced, with supplies on the first and second floors and exhausts in the bathrooms on the first and second floors. Both systems were turned off during all of the pressurization tests. The kitchen exhaust fan and dryer also were turned off, and their exterior vents were sealed.

(a) Floor transfer grille (b) Basement door (c) Access panel

FIG. 2 Photographs of smoke tests performed at NZERTF at the (a) floor transfer grilles, (b) basement door, and (c) access panel while depressurizing. Arrows indicate direction of airflow.

Because the NZERTF is airtight, the designers wanted to prevent the house from depressurizing when either the kitchen exhaust fan or dryer were turned on. Thus, a 15-cm round duct was installed in the attic, penetrating the exterior attic wall on the west side, with motorized and barometric dampers installed in the duct. The motorized damper was activated when either the kitchen exhaust fan or dryer was turned on. The barometric damper would open if the motorized damper was open and if the inside pressure was 10 Pa less than the outside pressure.

METHODOLOGY

The testing and data analysis methodologies as follows:

(1) Five house configurations were tested under various blower door arrangements.

(2) Each test configuration was expressed in mathematical form following the analogy of an electrical circuit with pressure corresponding to voltage and airflow corresponding to current. The airflow Q and pressure difference ΔP across a surface were represented by the equation $Q = C\Delta P^n$, where C is the flow coefficient ($m^3/s \bullet Pa$) and n is the pressure exponent. Both C and n were determined from the test data. These expressions formed the system of the equations needed to solve for the ELAs of the following building surfaces: roof (L_R), basement wall (L_{BW}), living area (first floor/second floor) walls (L_W), attic floor (L_{AF}), and basement ceiling leakage (L_{BC}) (illustrated in FIG. 3).

(3) The simultaneous solution of this system of equations resulted in values of C for each of the list building surfaces. C was converted to effective leakage, L, using the following equation

[24]:

$$L\,(\mathrm{cm}^2) \text{ at } \Delta P_{\mathrm{ref}} = C \bullet (\rho/2)^{0.5} \bullet (\Delta P_{\mathrm{ref}})^{n-0.5} \bullet 100^2 \tag{2}$$

where ΔP_{ref} is the reference differential pressure (Pa) and ρ is the density of air ($\mathrm{kg/m^3}$).

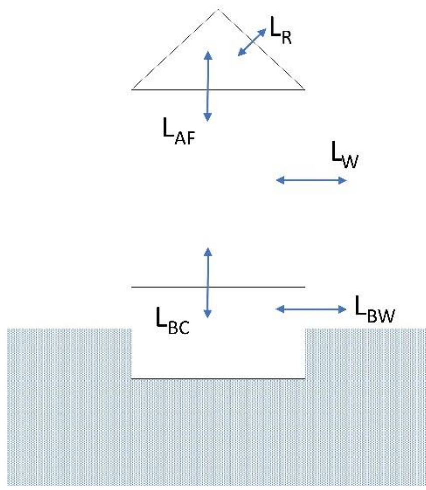

FIG. 3. Building surface leakages in NZERTF.

(4) The effective leakage of the basement door undercut and transfer grilles were determined by subtracting the result of the comparable "sealed" test configuration from the "unsealed" test result.

(1) Test Setup

Two blower doors, which complied with the requirements of ASTM E779-19, *Standard Test Method for Determining Air Leakage Rate by Fan Pressurization,* were used in the tests. Pressures were measured using a multichannel pressure measurement and fan control apparatus from the same manufacturer as the blower doors. Baseline pressures were recorded when the fan was turned off before and after each blower door test. These values were then averaged and subtracted from each measured pressure recorded during the test, as outlined in ASTM E779. The data logging and control software allowed for the simultaneous measurement of differential pressures across the fan and at three locations throughout the house. The software was setup to record differential pressures and fan flow rates between 10 Pa and 60 Pa in increments of 5 Pa, in both pressurization and depressurization modes. The software also provided the ability to take 100 pressure differential readings at each incremental differential pressure value and report the average. All tests were conducted over two weeks in November 2016, during which time the average indoor temperature was 21 °C, outdoor temperature was 7 °C and wind speed was 4 m/s.

(2) Test Configurations

Five house configurations were tested, varying the placement of the fan and open/closed status of exterior and interior doors (FIG. 4). All tests were successfully executed except for Test #3, which required the attic pressure to be at the same as the outside pressure. The existing opening in the attic (makeup-air duct) was not large enough to neutralize the attic-outdoor pressure. Details of each test and the mathematical expressions used to represent each test are described in the following sections.

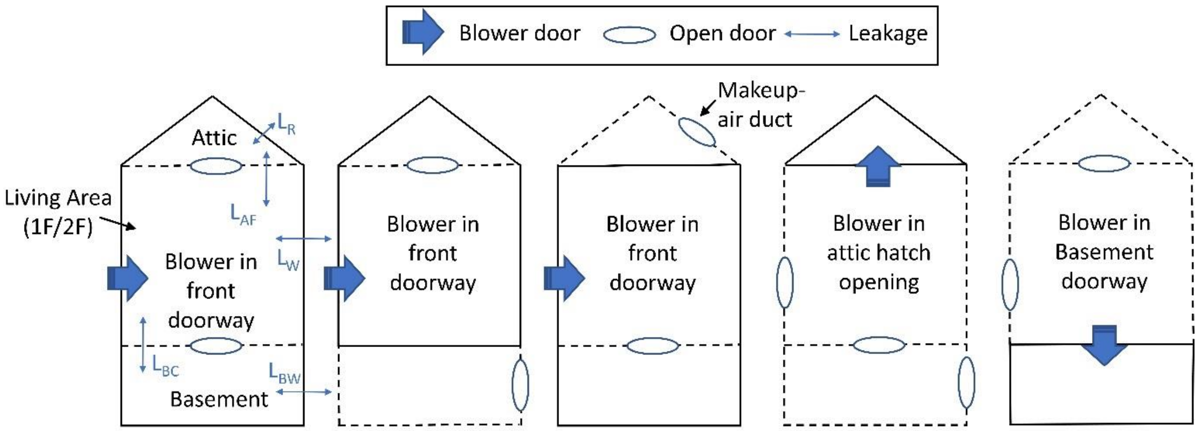

(a) Test #1 (b) Test #2 (c) Test #3 (d) Test #4 (e) Test #5

FIG. 4. Five house configurations for determining external and interzonal leakage.

Test #1

For this test configuration, the blower door was placed in the front doorway of the house, and both the basement door and attic hatch remained open. Pressure differentials with respect to the outdoors were measured in the basement, attic, and living room to ensure that the induced pressure across the building envelope was uniform across the entire house. Two subconfigurations ("A" and "B") were also tested: in Test #1A the exterior dryer and kitchen exhaust vents were unsealed and in Test #1B, these vents were sealed.

Test #1 was represented as an electrical circuit with three "resistances" (analogous to the flow coefficient C) in parallel (FIG. 5). The sum of the flow through each branch of the "circuit" is equal to Q_1, which was the measured airflow delivered by the blower door fan test to yield values of C_1 and n_1:

$$Q_1 = C_1 \Delta P_1^{n_1} = C_R \Delta P_{R_1}^{n_1} + C_W \Delta P_{W_1}^{n_1} + C_{BW} \Delta P_{BW_1}^{n_1} \tag{3}$$

Note that the value of n_1 is assumed to be the same for all surfaces in Eq. (3). No tests were performed to determine these values of *n* individually as part of Test #1. The subscript 1 denotes Test #1, and subscripts R, BW, and W denote the building surfaces (roof, basement wall and walls, respectively). On the basis of consideration of the similarity in airtightness of the exterior surfaces throughout the house, and the inability to measure them separately, we assumed that the following relationship:

$$C_R/A_{roof} = C_{BW}/A_{basement\ wall} = C_W/A_{walls} \tag{4}$$

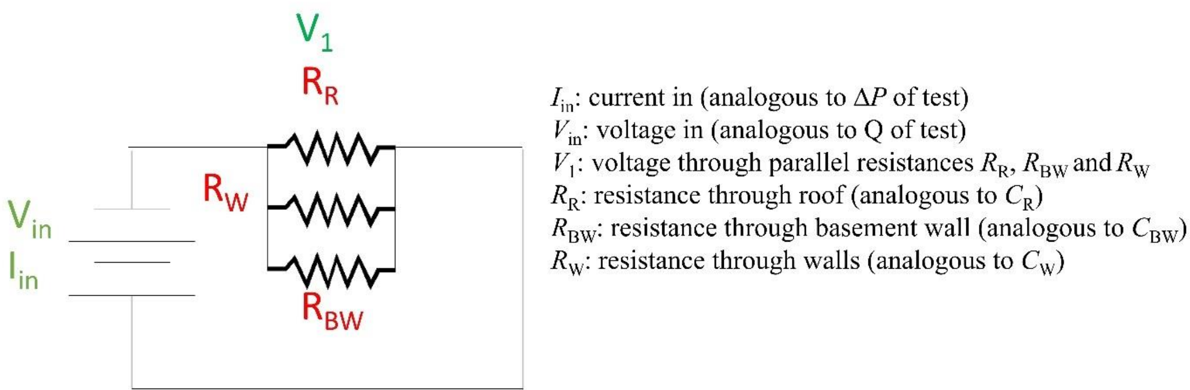

FIG. 5. Electrical circuit equivalent of Test #1

Test #2

For this test configuration, the blower door was placed in the front doorway. The basement door was closed and the attic hatch was opened. Four subconfigurations (A, B, C, and D) were tested, varying the sealing and unsealing of the first floor transfer grilles (between the first floor and the basement) and the sealing and unsealing of the basement door undercut as summarized in Table 2.

TABLE 2. Summary of subconfigurations for Test #2

Test #2 subconfigurations	First floor transfer grilles	Basement door undercut
A	Unsealed	Unsealed
B	Sealed	Unsealed
C	Unsealed	Sealed
D	Sealed	Sealed

Test #2 also has three resistances in parallel (C_R, C_W, C_2), with one of the resistances (C') composed of two resistances in series (C_{BW}, C_{BC}) (FIG. 6). Because the basement window is open for Test #2, the resistance R_B is essentially zero. The sum of the airflow through each branch of the "circuit" is equal to Q_2, which was measured during the blower door tests and yielded values of C_2 and n_2. The airflow-pressure expressions are as follows, where the subscript 2 refers to Test #2. Note that the value of n_2 is assumed to be the same for all surfaces in Eqs. (5) and (6).

$$Q_2 = C_2 \Delta P_2^{n_2} = C' (\Delta P')^{n'} + C_W \Delta P_{W_2}^{n_2} + C_R \Delta P_{R_2}^{n_2}, \text{ and} \tag{5}$$

$$C'(\Delta P')^{n'} = C_{BC} \Delta P_{BC_2}^{n_2} \tag{6}$$

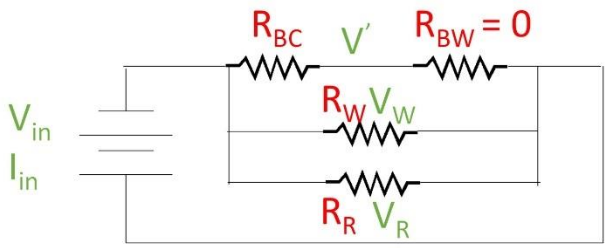

I_{in}: current in (analogous to ΔP of test)
V_{in}: voltage in (analogous to Q of test)
V_{R}: voltage through R_{R}
V_{W}: voltage through R_{W}
V': voltage through combined R_{BW} and R_{BC}
R_{R}: resistance through roof (analogous to C_{R})
R_{BW}: resistance through basement wall (analogous to C_{BW})
R_{W}: resistance through walls (analogous to C_{W})
R_{BC}: resistance through basement ceiling (analogous to C_{BC})

FIG. 6. Electrical circuit equivalent of Test #2.

Test #3

In Test #3, the blower door was placed in the front doorway. The basement door was open and the attic hatch was closed. Two subconfigurations (A and B) were tested: in Test #3A the attic transfer grilles (between the second floor and attic) were unsealed and in Test #3B, these transfer grilles were sealed. The airflow-pressure expressions are as follows:

$$Q_3 = C_3 \Delta P_3^{n_3} = C^{'}(\Delta P^{'})^{n^{'}} + C_W \Delta P_{W_3}^{n_3} + C_{BW} \Delta P_{BW_3}^{n_3} \tag{7}$$

$$C'(\Delta P')^{n'} = C_R \Delta P_{R_3}^{n_3} = C_{AF} \Delta P_{AF_3}^{n_3} \tag{8}$$

Note that the value of n_3 is assumed to be the same for all surfaces in Eqs. (7) and (8).

Test #4

In Test #4, a smaller fan designed for duct leakage tests was connected to the attic hatch opening using a plywood mount and flexible duct (FIG. 7), and the front door of the house was open. Four subconfigurations (A, B, C, and D) were tested, alternating sealing and unsealing of the attic transfer grilles (between the second floor and the attic) and makeup-air duct in the attic (Table 3).

The airflow-pressure expression is as follows:

$$Q_4 = C_4 \Delta P_4^{n_4} = C_R \Delta P_{R_4}^{n_4} + C_{AF} \Delta P_{AF_4}^{n_4} \tag{9}$$

Note that the value of n_4 is assumed to be the same for all surfaces in Eq. (9).

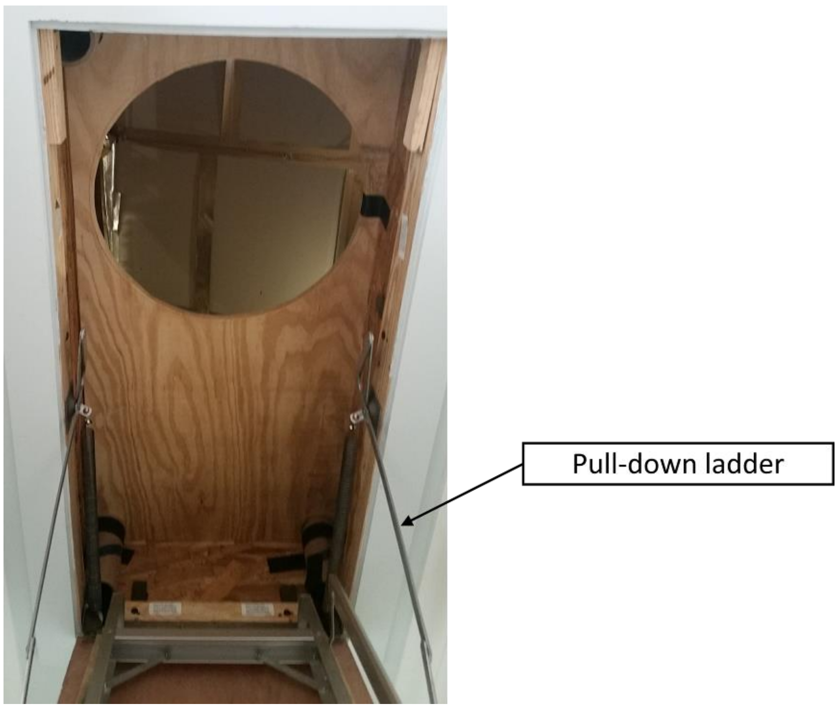

FIG. 7. Plywood mount for smaller fan in attic hatch opening.

TABLE 3. Summary of subconfigurations for Test #4.

Test #4 subconfigurations	**Attic transfer grilles**	**Makeup-air duct**
A	Sealed	Unsealed
B	Unsealed	Unsealed
C	Sealed	Sealed
D	Unsealed	Sealed

Test #5

For Test #5, the blower door was placed in the basement doorway and the front door of the house was open. Two subconfigurations (A and B) were tested: in Test #5A the first floor transfer grilles were sealed and in Test #5B, these transfer grilles were unsealed. The airflow-pressure expression is as follows:

$$Q_5 = C_5 \Delta P_5^{n_5} = C_{BW} \Delta P_{BW_5}^{n_5} + C_{BC} \Delta P_{BC_5}^{n_5} \tag{10}$$

Note that the value of n_5 is assumed to be the same for all surfaces in Eq. (10).

(3) Determining Leakage Values of Building Surfaces

This section describes the determination of the individual leakage values from the results of the tests that were just described, solving for C_R, C_{BW}, C_W, C_{AF}, and C_{BC}. Using the assumption expressed in Eq. (4), the only unknowns were C_{AF} and C_{BC}. They were solved, respectively, using Eq. (9) for Test #4C and Eq. (10) for Test #5A. These test numbers were the subconfigurations in which the interior leakage paths (basement door undercut and transfer grilles) were sealed. The values of C_R, C_{BW}, C_W, C_{AF} and C_{BW} were then converted to effective leakages L using Eq. (2).

The values of L_{AF} and L_{BC} determined using C_{AF} and C_{BC}, respectively, were compared with values calculated by subtracting the result of the comparable "sealed" test configuration from the "unsealed" test result. The ELA of Test #5A (first floor transfer grilles sealed) minus the leakage area of the basement wall (L_{BW}) equals the leakage area of the basement ceiling (L_{BC}). The ELA of Test #4C (attic transfer grilles sealed) minus the leakage area of the roof (L_R) equals the leakage area of the attic floor (L_{AF}).

(4) Determining Leakage Values of Basement Door Undercut and Transfer Grilles

The leakages of the basement door undercut and transfer grilles were determined by subtracting the result of the comparable "sealed" test configuration from the "unsealed" test result. The solution process for each building component is described below:

The effective leakage of the basement door undercut was calculated two ways:

(1) ELA Test #2 with first floor transfer grilles unsealed: ELA_{2A} (door undercut unsealed) minus ELA_{2C} (door undercut sealed)

(2) ELA Test #2 with first floor transfer grilles sealed: ELA_{2B} (door undercut unsealed) minus ELA_{2D} (door undercut sealed).

The effective leakage of the first floor transfer grilles was calculated three ways:

(1) ELA Test #2 basement door undercut unsealed: ELA_{2A} (transfer grilles unsealed) minus ELA_{2B} (transfer grilled sealed)

(2) ELA Test #2 basement door undercut sealed: ELA_{2C} (transfer grilles unsealed) minus ELA_{2D} (transfer grilled sealed)

(3) ELA_{5A} (transfer grilles unsealed) minus ELA_{5B} (transfer grilles sealed)

The effective leakage of the attic transfer grilles was calculated two ways:

(1) ELA Test #4 makeup-air duct sealed: ELA_{4A} (transfer grilles unsealed) minus ELA_{4B} (transfer grilled sealed)

(2) ELA Test #4 makeup-air duct unsealed: ELA_{4C} (transfer grilles unsealed) minus ELA_{4D}

(transfer grilled sealed).

RESULTS

This section summarizes the ELAs obtained from the 14 blower door tests. These ELAs are used to calculate the leakiness of the roof, first and second floor walls, basement walls, basement ceiling, and attic floor using derived flow coefficients. The test ELAs also are used to calculate the effective leakages of the basement door undercut and transfer grilles. Lastly, results from multizone airflow simulations of the NZERTF, using the calculated leakages as inputs, are presented.

Effective leakages

The ELA at 50 Pa for all 14 tests were calculated using the procedures outlined in ASTM E779 (TABLE 4). The results are listed by test configuration (Test #1 to Test #5) and subconfiguration denoting whether vents and other openings were sealed or unsealed. Because of the attic-outdoor pressure not being able to be neutralized, the results of Tests #3A and #3B actually captured the leakage of the basement wall, first and second floor walls, and the combined leakage of the attic floor and roof. With the attic floor being so leaky relative to the attic roof (see TABLE 5 and subsequent explanation), Test #3 results closely matched the results of Test #1B, which captured the combined leakage of basement wall, first and second floor walls, and attic roof. (The exterior dryer and kitchen exhaust vents were sealed during these three tests.) For Tests #1 and #3, n = 0.65 on average, ranging from n = 0.64 to n = 0.67.

As expected, the ELAs of Tests #2, #4, and #5 (which include the combined leakage of exterior and interior leakages) are greater than the ELAs of Test #1 (exterior envelope only) because attention was paid to minimizing the leakiness of the exterior envelope. No attention was paid to the leakiness of the basement ceiling or attic floor, which is reasonable because both the basement and attic are within the conditioned volume. The ELAs of Test #4 were the highest of the tests, which indicated that the attic floor was leakier than the basement ceiling. This was also verified by further analysis presented below. For Tests #2, #4, and #5, n = 0.61 on average (ranging from n = 0.58 to n = 0.68), which was smaller than the average of the n values for Tests #1 and #3 (tests of the exterior envelope leakage).

TABLE 4. Summary of ELA at 50 Pa for five test configurations and their subconfigurations.

Test number	Leakage determined	ELA at 50 Pa (cm²)	95 % confidence interval (+/- cm²)
1A	L_R+L_{BW}+L_W (vents unsealed)	**237**	7
1B	L_R+L_{BW}+L_W (vents sealed)	**200**	3
2A	L_R+L_W + (L_{BW} + L_{BC})[1]	**898**	12
2B	L_R+L_W + (L_{BW} + L_{BC})[1]	**676**	9
2C	L_R+L_W + (L_{BW} + L_{BC})[1]	**765**	8
2D	L_R+L_W + (L_{BW} + L_{BC})[1]	**539**	9
3A	L_{BW}+L_W + (L_R + L_{AF})[1]	**202**	4
3B	L_{BW}+L_W + (L_R + L_{AF})[1]	**204**	3
4A	L_R + L_{AF}[1]	**696**	16
4B	L_R + L_{AF}[1]	**914**	51
4C	L_R + L_{AF}[1]	**694**	17
4D	L_R + L_{AF}[1]	**941**	30
5A	L_{BW} + L_{BC} (first floor grilles sealed)	**611**	4
5B	L_{BW} + L_{BC} (first floor grilles unsealed)	**836**	6

1. See the section, “Test Configurations”, for descriptions of the various subconfigurations.

As discussed in the section, “Methodology”, the ELAs of the tests are used to calculate C and L of the various building components (i.e., roof, walls, floor). The values of C_R, C_{BW}, and C_W were converted to effective leakages, L, using Eq. (1) and then normalized by their respective surface areas in TABLE 1. The assumption in Eq. (4), $L'_R = L'_W = L'_{BW}$, where the prime notation indicating

L is normalized by surface area, is given in TABLE 5. TABLE 5 also shows the results of calculating L_{AF} and L_{BC} two ways, (1) by determining C_{AF} and C_{BW} and then converting to L and (2) by subtracting the result of the comparable "sealed" test configuration from the "unsealed" test result. TABLE 5 shows the average calculated L_{AF} = 618 cm^2 at 50 Pa (95 % confidence interval (CI) 567 cm^2 to 655 cm^2) when calculated using C_{AF} and shows that the average calculated L_{AF} = 606 cm^2 at 50 Pa (95 % CI 596 cm^2 to 620 cm^2) when calculated using $ELA_{4C} - L_{R.}$ There was only a 2 % difference in L_{AF} calculated by these two methods.

TABLE 5 shows the average calculated L_{BC} = 614 cm^2 at 50 Pa (95 % CI 594 cm^2 to 634 cm^2) when calculated using C_{BC} and shows the average calculated L_{BC} = 611 cm^2 at 50 Pa (95 % CI 596 cm^2 to 620 cm^2) when calculated using $ELA_{5A} - L_{BW}$ (< 1 % difference). The last column of TABLE 5 shows the effective leakages normalized by their respective surface area or per item. The attic floor (4.66 cm^2/m^2 at 50 Pa) is about 15 % leakier than the basement ceiling (4.01 cm^2/m^2 at 50 Pa) The attic floor and basement ceiling are also about 10 times leakier than the exterior envelope (0.48 cm^2/m^2 at 50 Pa). The leakage area of the attic floor (606 cm^2 at 50 Pa) is greater than the leakage of the attic transfer grilles (233 cm^2 at 50 Pa). The leakage of the basement ceiling (611 cm^2 at 50 Pa) is greater than the leakage of the first floor transfer grilles (224 cm^2 at 50 Pa).

TABLE 5. Flow coefficient and calculated leakages of building components.

	C (m^3/s•Pa)	**L from Eq. (2) (cm^2)**	**L using $ELA_{Test\#}$ (cm^2)**	**L' (cm^2/m^2 or per item)**
Roof	C_R=0.006	L_R=88	N/A	0.48 cm^2/m^2
Basement wall	C_{BW}=0.00005	L_{BW}=1		0.48 cm^2/m^2
First and second floor walls	C_W=0.010	L_W=150		0.48 cm^2/m^2
Attic floor	C_{AF}=0.041	L_{AF}=618	$L_{AF}=ELA_{4C} - L_R$ = 606	4.66 cm^2/m^2
Basement ceiling	C_{BC}=0.049	L_{BC}=614	$L_{BC}=ELA_{5A} - L_{BW}$ = 611	4.05 cm^2/m^2

Basement door undercut	N/A	N/A	$ELA_{2A} – ELA_{2C}$ = 132 $ELA_{2B} – ELA_{2D}$ = 137	135 cm^2
First floor transfer grilles (qty = 3)	N/A	N/A	$ELA_{2A} – ELA_{2B}$ = 221 $ELA_{2C} – ELA_{2D}$ = 226 $ELA_{5A} – ELA_{5B}$ = 225	75 cm^2 per transfer grille
Attic transfer grilles (qty = 2)	N/A	N/A	$ELA_{4A} – ELA_{4B}$ = 218 $ELA_{4C} – ELA_{4D}$ = 248	116 cm^2 per transfer grille

SIMULATIONS

To evaluate the effects of different ventilation strategies on airflows and contaminant concentrations in the NZERTF, the L' at 50 Pa (cm^2/m^2 or per item) in TABLE 5 were input into a multizone airflow model of the house developed using CONTAM [26]. This CONTAM model was also coupled with EnergyPlus, a whole-building energy analysis tool, to study the energy implications of these airflows [27]. In a previous modeling study, preliminary estimates of the interzone leakage values were used to predict formaldehyde and acetaldehyde concentrations [28].

The CONTAM model considers the interaction between external forces driving airflow (inside-outside temperature difference and wind) and building heating, ventilating, and air conditioning (HVAC) system airflow rates to determine pressures and airflows across internal partitions and the building envelope. CONTAM also accounts for external and internal contaminant sources and removal mechanisms to calculate contaminant transport associated with the airflows. EnergyPlus implements a multizone heat transfer model that accounts for conductive, convective and radiant heat transfer associated with building materials; interzone and envelope airflows; and HVAC systems. During cosimulation using the coupled model, indoor air temperatures and HVAC system airflow rates are passed from EnergyPlus to CONTAM, and airflow rates across the building envelope and between internal zones are passed from CONTAM to EnergyPlus [29, 30]. Details on the model and simulated concentrations of formaldehyde and acetaldehyde in the NZERTF are given in .

Simulations were performed using preliminary estimates for the interzonal leakages that were based on engineering judgement for the floor leakage and manufacturer's catalogs (for the transfer grilles), before the measurements reported on in this paper were performed. The preliminary floor leakage value underestimated the measured value by about half, and the effective leakage value of the transfer grilles had been overestimated by a factor of about three (TABLE 6). Simulations were then repeated using the measured interzonal leakage values. Annual simulations were performed using the Typical Meteorological Year 3 (TMY3) weather file for Baltimore, MD [31], with a time step of 1.0 min and with the heat pump fan controlled by the thermostat (set to 21.1 °C in the heating season and 23.9 °C in the cooling season) and the HRV running continuously at 0.05 m^3/s. Simulations were also performed with both the heat pump fan and HRV off.

TABLE 6. Preliminary and measured leakages of building components.

	Preliminary leakage	***Measured leakage***
Attic floor	2 cm^2/m^2 at 50 Pa	4.66 cm^2/m^2 at 50 Pa
Basement ceiling	2 cm^2/m^2 at 50 Pa	4.05 cm^2/m^2 at 50 Pa
Attic transfer grilles (qty=2)	418 cm^2 /each	116 cm^2/each
First floor transfer grilles (qty=3)	232 cm^2 /each	75 cm^2/each
Basement door undercut	229 cm^2	135 cm^2

TABLE 7 shows that there were significant differences in the predicted airflow rates of the individual paths (averaged over the annual simulation). On average, the predicted flow through the basement ceiling and attic floor using the measured leakage was higher than the value using the preliminary leakage. In contrast, the predicted flow through attic, first floor transfer grilles, and basement door undercut using the measured leakage were lower using the preliminary leakage. Note that the total airflow from the basement to the first floor, and from the second floor to the attic, were the same for the preliminary and measured leakage when averaged over a year (differences < 0.5 %). It may be that no change was observed in the average interzonal airflow because the exterior building leakage was comparatively airtight (ten times more airtight) and changes to the interzonal leakage were not great enough to affect the overall airflow pattern within the house.

The heat pump system was 100 % recirculating and the HRV was balanced. Although there were only heat pump supplies in the basement (no returns), whether the systems were on or off, the total infiltration was the same. With the systems off (details not shown for brevity), the airflow from the basement to the first floor decreased by 4 % because the heat pump was no longer supplying air to the basement. The only outside air supplied to the basement, when the heat pump and HRV was off, would have been through the basement wall, which had an ELA of 1 cm^2 at 50 Pa (0.48 cm^2/m^2 multiplied by the wall area of 2 m^2). With the systems off, the airflow from the second floor to the attic increased by 25 % to balance the decrease of air from the basement to the first floor.

TABLE 7. Predicted interzonal airflow rates using preliminary and measured leakage averaged over a year

Interzonal airflow rates (systems on)	**Average flow using preliminary leakage (m^3/s)**	**Average flow using measured leakage (m^3/s)**	**Percentage difference**
Attic transfer grilles	3.4E-03	9.7E-04	-72 %
Attic floor	1.8E-03	4.2E-03	139 %
First floor transfer grilles	5.3E-05	2.2E-05	-58 %
Basement ceiling	8.2E-06	4.2E-05	415 %
Basement door undercut	3.7E-05	3.4E-05	-9 %
Airflow from second floor to attic	5.2E-03	5.2E-03	-0.11%
Airflow from basement to first floor	9.9E-05	9.9E-05	0.06%

The average simulated concentrations of formaldehyde were not significantly different between using the preliminary and measured interzonal leakage. The differences in the average annual concentrations were < 0.05 % in the basement, combined first and second floor, and attic. This was because the total interzonal airflow between the basement and first floor, and between the second floor and the attic, averaged over a year, did not change whether using the preliminary or measured leakage. The similarity in the simulated formaldehyde concentrations also could have been due to the nature of the entire house being within the conditioned space. In a house with typical-construction, a leaky attic floor (coupled with a vented attic that is not part of the conditioned space) may create a greater stack effect within the house and may redistribute contaminants differently than in the NZERTF. The fact that the interzonal leakage did not affect the distribution of formaldehyde in the NZERTF could have been attributed to the heat pump system recirculating air from the house and delivering it to the basement and the house.

DISCUSSION

One challenge during this series of blower door tests was not being able to neutralize the pressure across the attic roof. Unsuccessful attempts were made to conduct a two-blower test by manually adjusting the speed of the blower door in the front doorway and smaller fan in the attic hatch opening. The authors will attempt a two-blower test using additional fan control devices in the future.

Blower door test results showed that the interior floors were approximately 10 times leakier than the exterior building envelope and that the leakage associated with the transfer grilles between levels was less than the total floor leakage. Considering that all the levels of the NZERTF were all within the conditioned space, the leaky interior floors do not pose an energy penalty (i.e., cold air from the basement flowing up to house, and conditioned air from house flowing out through the roof) when paired with a tight exterior envelope. In a home of more typical construction, however, in which the attic is not within the conditioned space and the exterior walls are not as tight, there could be a significant energy penalty as conditioned air escapes to the attic and out the roof vents.

There were no significant differences in the total interzonal airflows between the levels of the NZERTF, and no significant differences in the simulated formaldehyde concentrations, using preliminary and measured interzonal leakage in the NZERTF (both averaged over a year). Reasons for this lack of difference in the annual averages may include the fact that the zones within the NZERTF were all within the conditioned envelope. Thus cold basements and hot attics did not create as great a stack effect as created in homes with only living areas within the conditioned space. Also, the heat pump in the NZERTF recirculated air between the basement, first floor, and second floor, which may not be the case in all homes. Last, as noted, no change was observed in the average interzonal airflow because the exterior building leakage was comparatively airtight (10 times more airtight) and changes to the interzonal leakage were not great enough to affect the overall airflow pattern within the house. Nevertheless, improved knowledge of interzonal leakage could improve estimates of contaminant transport in other homes, especially when considering transient effects. These findings will be compared with the results of interzonal tracer decay tests, which have been performed in the NZERTF but not yet analyzed.

CONCLUSION

The NZERTF is a 250 m^2 two-story, unoccupied test home located at NIST in Gaithersburg, MD. It is airtight (0.6 h^{-1} at 50 Pa) and has a highly insulated building enclosure designed for heat, air and moisture control. Because the basement, first floor, second floor, and attic levels are all within the conditioned space, no special attention has been given to the airtightness of the interior floors; however, to support airflow modeling efforts, this leakage was quantified through a series of interzonal pressurization tests. It was found that the interior floors were 10 times leakier than the exterior building envelope, and that the leakage associated with the transfer grilles between levels was less than the total floor leakage. This paper described the design of the interzonal tests and the challenges to perform them. Having more accurate estimates of interzonal leakage could be advantageous in understanding the transport of air and contaminants in multizone structures, especially with respect to transient effects.

List of Figure Captions

FIG. 1. NZERTF at NIST facing south.
FIG. 2 Photographs of smoke tests performed at NZERTF at the (a) floor transfer grilles, (b) basement door, and (c) access panel while depressurizing.
FIG. 3. Building surface leakages in NZERTF.
FIG. 4. Five house configurations for determining external and interzonal leakage.
FIG. 5. Electrical circuit equivalent of Test #1
FIG. 6. Electrical circuit equivalent of Test #2.
FIG. 7. Plywood mount for smaller fan in attic hatch opening.

TABLE 1. Physical characteristics of NZERTF

TABLE 2. Summary of subconfigurations for Test #2
TABLE 3. Summary of subconfigurations for Test #4.
TABLE 4. Summary of ELA at 50 Pa for five test configurations and their subconfigurations.
TABLE 5. Flow coefficient and calculated leakages of building components.

REFERENCES

REFERENCES

1. U.S. Energy Information Administration, ed., *Annual Energy Outlook 2018 with Projections to 2050* (Washington, DC: U.S. Energy Information Administration, 2018), 127.
2. *Windows and Building Envelope Research and Development: Roadmap for Emerging Technologies*" (Washington, DC: U.S. Department of Energy, 2014).
3. *Energy Standard for Buildings Except Low-Rise Residential Buildings*, ANSI/ASHRAE/IES Standard 90.1-2016 (Atlanta, GA: American Society of Heating, Refrigerating and Air-Conditioning Engineers, 2016).
4. *U.S. Army Corps of Engineers Air Leakage Test Protocol for Building Envelopes* (Chapaign, IL: U.S. Army Corps of Engineers Research and Development Center, 2012).
5. *International Energy Conservation Code* (Washington, DC: International Code Council, 2015).
6. M. Jayjock and A. A. Havics, "Residential Inter-Zonal Ventilation Rates for Exposure Modeling," *Journal of Occupational and Environmental Hygiene* 15, no. 5 (2018): 376–388, http://doi.org/10.1080/15459624.2018.1438615
7. S. J. Emmerich, J. E. Gorfain, and C. Howard-Reed, "Air and Pollutant Transport from Attached Garages to Residential Living Spaces–Literature Review and Field Tests," *International Journal of Ventilation* 2, no. 3 (2003): 265–276, http://doi.org/10.1080/14733315.2003.11683670
8. L. Du, S. Batterman, C. Godwin, J.-Y. Chin, E. Parker, M. Breen, W. Brakefield, T. Robins, and T. Lewis, "Air Change Rates and Interzonal Flows in Residences, and the Need for Multi-Zone Models for Exposure and Health Analyses," *International Journal of Environmental Research and Public Health* 9, no. 12 (2012): 4639–4662, http://doi.org/10.3390/ijerph9124639
9. E. L. Hult, M. H. Sherman, I. S. and Walker, "Blower-Door Techniques for Measuring Interzonal Leakage" (paper presentation, *Buildings XII*, Lawrence Berkeley National Laboratory, Berkeley, CA, December 4-6, 2013).
10. C. F. A. Afonso, E. A. B. Maldonado, and E. Skåret, "A Single Tracer-Gas Method to Characterize Multi-Room Air Exchanges," *Energ Buildings* 9, no. 4 (1986): 273–280.
11. F. D. Heidt, R. Rabenstein, and G. Schepers, "Comparison of Tracer Gas Methods for Measuring Airflows in Two-zone Buildings," *Indoor Air* 1, no. 3 (1991): 297–309.
12. S. L. Miller, K. Leiserson, and W. W. Nazaroff, "Nonlinear Least-Squares Minimization Applied to Tracer Gas Decay for Determining Airflow Rates in a Two-Zone Building," *Indoor Air* 7, no. 1 (1997): 64–75, http://doi.org/doi:10.1111/j.1600-0668.1997.t01-1-00008.x

13. P. J. O'Neill and R. R. Crawford, "Identification of Flow and Volume Parameters in Multi-Zone Systems Using a Single-Gas Tracer Technique," *ASHRAE Transactions* 1991, no. 1 (1997): 49–54.
14. M. Enai, N. Aratani, C. Y. Shaw, and J. T. Reardon (1993). Differential and integral method for computing interzonal airflows using multiple tracer gases. *Proceedings of International Symposium on Room Air Convection and Ventilation Effectiveness (ISRACVE), 22-24 July, 1992 Tokyo, Japan, Atlanta: ASHRAE*, 357-362.
15. R. P. Sieber, R. W. Besant, and G. J. Schoenau, "Variations in Interzonal Airflow Rates in a Detached House Using Tracer Gas Techniques" r presentation, *ASHRAE Transactions* 99, (1993): 699–708.
16. L. Du, S. Batterman, C. Godwin, Z. Rowe, and J. Y. Chin, "Air Exchange Rates and Migration of VOCs in Basements and Residences," *Indoor Air* 25, no. 6 (2015): 598–609, http://doi.org/10.1111/ina.12178
17. A. H. Fanney, V. Payne, T. Ullah, L. Ng, M. Boyd, F. Omar, M. Davis, H. Skye, B. Dougherty, B. Polidoro, W. Healy, J. Kneifel, and B. Pettit, "Net-Zero and Beyond! Design and Performance of NIST's Net-Zero Energy Residential Test Facility," *Energy and Buildings* 101, no. 15 (2015): 95–109, http://doi.org/10.1016/j.enbuild.2015.05.002
18. F. Omar and S. T. Bushby, "Simulating Occupancy in the NIST Net-Zero Energy Residential Test Facility" (Gaithersburg, MD: National Institute of Standards and Technology, 2013).
19. L. Ng, A. Persily, and S. Emmerich (2015), “Infiltration and Ventilation in a Very Tight, High Performance Home” *Proceedings of 36th AIVC Conference Effective Ventilation High Performance Buildings*, Madrid, Spain, September 23–24, 2015, Brussels: AIVC, 719–726.
20. *LEED BD+C: Homes, v4*, LEED v4 (Washington, DC: U.S. Green Building Council, 2014).
21. *ENERGY STAR Certified Homes, Version 3.1* (Rev. 06) (Washington, DC: U.S. Environmental Protection Agency, 2015).
22. *PHIUS + 2015: Passive Building Standard–North America*" (Chicago, IL: Passive House Institute US, 2015).
23. W. R. Chan, J. Joh, and M. H. Sherman, "Analysis of Air Leakage Measurements of US Houses," *Energy and Buildings* 66 (November 2013): 616–625, http://doi.org/10.1016/j.enbuild.2013.07.047
24. *ASHRAE Handbook Fundamentals* (Atlanta, GA: American Society of Heating, Refrigerating and Air-Conditioning Engineers, 2017).
25. *Standard Test Method for Determining Air Leakage Rate by Fan Pressurization* ASTM E779-19 (West Conshohocken, PA: ASTM International, 2019), www.astm.org
25. B. Pettit, C. Gates, A. H. Fanney, and W. Healy, "Design Challenges of the NIST Net-Zero Energy Residential Test Facility" (Gaithersburg, MD: National Institute of Standards and Technology, 2014)..
26. W. S. Dols and B. Polidoro, "CONTAM User Guide and Program Documentation" (Gaithersburg, MD: National Institute of Standards and Technology, 2016).
27. *EnergyPlus 8.4* (Washington, DC: U.S. Department of Energy, 2015).
28. L. Ng, D. Poppendieck, W. S. Dols, and S. J. Emmerich, "Evaluating Indoor Air Quality and Energy Impacts of Ventilation in a Net-Zero Energy House Using a Coupled Model,"

Science and Technology for the Built Environment 24, no. 2 (2017): 124–134, https://doi.org/10.1080/23744731.2017.1401403

29. W. S. Dols, S. J. Emmerich, and B. J. Polidoro, "Coupling the Multizone Airflow and Contaminant Transport Software CONTAM with EnergyPlus Using Co-simulation," *Building Simulation* 9 (2016): 469–479, http://doi.org/10.1007/s12273-016-0279-2
30. M. Wetter, "Co-simulation of Building Energy and Control Systems with the Building Controls Virtual Test Bed," *Journal of Building Performance Simulation* 4, no. 3 (2011): 185–203, http://doi.org/10.1080/19401493.2010.518631
31. "National Solar Radiation Data Base: 1991–2005 Update: Typical Meteorological Year 3," (Lakewood, CO: National Renewable Energy Laboratory, 2015).